HHS Public Access

Author manuscript

Cell Rep. Author manuscript; available in PMC 2022 August 29.

Published in final edited form as:

Cell Rep. 2022 July 19; 40(3): 111098. doi:10.1016/j.celrep.2022.111098.

Direct type I interferon signaling in hepatocytes controls malaria

Camila Marques-da-Silva[1,2], **Kristen Peissig**[1,2], **Michael P. Walker**[3], **Justine Shiau**[2,4], **Carson Bowers**[2], **Dennis E. Kyle**[1,2,4], **Rahul Vijay**[5], **Scott E. Lindner**[3], **Samarchith P. Kurup**[1,2,6,*]

[1]Department of Cellular Biology, University of Georgia, Athens, GA, USA

[2]Center for Tropical and Emerging Global Diseases, University of Georgia, Athens, GA, USA

[3]Department of Biochemistry and Molecular Biology, The Huck Center for Malaria Research, Pennsylvania State University, University Park, PA, USA

[4]Department of Infectious Diseases, University of Georgia, Athens, GA, USA

[5]Center for Cancer Cell Biology, Immunology and Infection, Rosalind Franklin University of Medicine and Science, North Chicago, IL, USA

[6]Lead contact

SUMMARY

Malaria is a devastating disease impacting over half of the world's population. *Plasmodium* parasites that cause malaria undergo obligatory development and replication in hepatocytes before infecting red blood cells and initiating clinical disease. While type I interferons (IFNs) are known to facilitate innate immune control to *Plasmodium* in the liver, how they do so has remained unresolved, precluding the manipulation of such responses to combat malaria. Utilizing transcriptomics, infection studies, and a transgenic *Plasmodium* strain that exports and traffics Cre recombinase, we show that direct type I IFN signaling in *Plasmodium*-infected hepatocytes is necessary to control malaria. We also show that the majority of infected hepatocytes naturally eliminate *Plasmodium* infection, revealing the potential existence of anti-malarial cell-autonomous immune responses in such hepatocytes. These discoveries challenge the existing paradigms in *Plasmodium* immunobiology and are expected to inspire anti-malarial drugs and vaccine strategies.

Graphical abstract

*Correspondence: samar@uga.edu.

AUTHOR CONTRIBUTIONS

C.M.-d.-S., K.P., M.P.W., J.S., C.B., R.V., S.E.L., and S.P.K. designed, performed, or analyzed the experiments. S.E.L. and D.E.K. provided vital resources. C.M.-d.-S. and S.P.K. wrote the manuscript.

SUPPLEMENTAL INFORMATION

Supplemental information can be found online at https://doi.org/10.1016/j.celrep.2022.111098.

DECLARATION OF INTERESTS

The authors declare no competing interests.

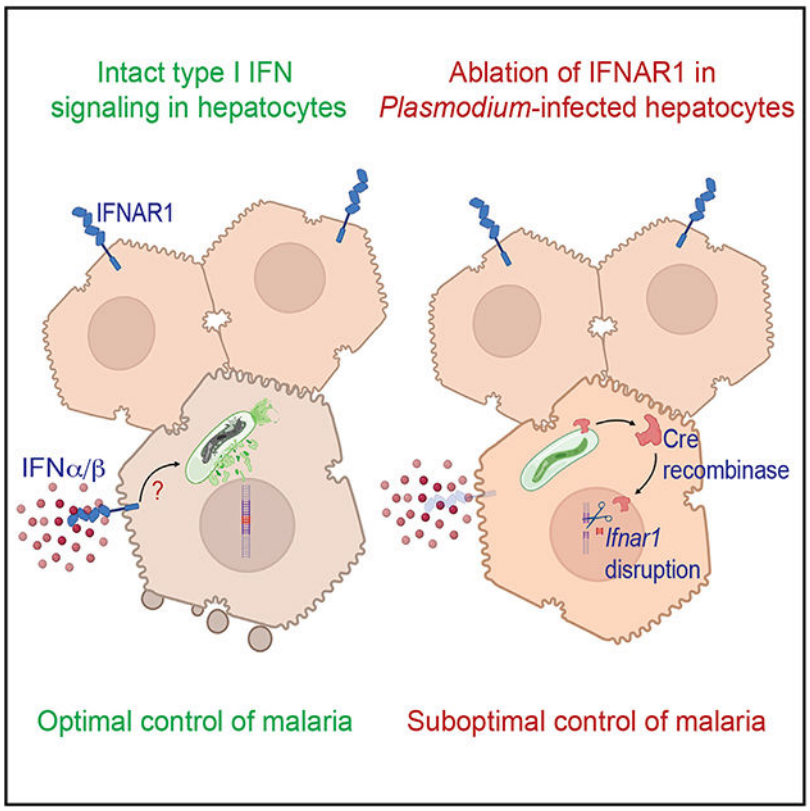

In brief

Utilizing a transgenic *Plasmodium* strain expressing Cre recombinase that selectively ablates type I IFN receptor in only the infected hepatocytes, Marques-da-Silva et al. show that direct type I IFN signaling in the infected hepatocytes is both necessary and sufficient to control liver-stage malaria.

INTRODUCTION

Clinical malaria infections caused by *Plasmodium* parasites are responsible for the death and suffering of millions of people around the world (WHO, 2019). The sporozoite stage of *Plasmodium* inoculated into humans by *Anopheles* mosquitoes has to undergo developmental transformation and replication in hepatocytes (constituting the “liver stage” of malaria) before infecting red blood cells and causing the symptomatic and dangerous “blood stage” of malaria (Cowman et al., 2016). The blood stage is exclusively responsible for all the morbidity and mortality associated with malaria, as well as its transmission. Therefore, limiting the progression of *Plasmodium* beyond the liver is the primary goal of the majority of current strategies aimed at controlling or eradicating malaria (Mo and McGugan, 2018; Mo et al., 2020). However, a major impediment to such approaches is how little we know about the nature of host responses to *Plasmodium* infection in the liver (Gazzinelli et al., 2014). Type I interferons (IFNs) are the primary mediators of innate immune control of liver-stage malaria (Gazzinelli et al., 2014; Liehl et al., 2014; Miller et al., 2014). There is increasing evidence that limiting *Plasmodium* infection in

the liver by induction of type I IFNs blunts the extent and impact of clinical malaria (He et al., 2020). However, how type I IFNs drive the control of *Plasmodium* in the liver has remained unresolved (Liehl et al., 2014; Miller et al., 2014). Currently, it is presumed that type I IFNs produced by *Plasmodium*-infected hepatocytes facilitate the recruitment of immune cells from circulation either through direct signaling or through the induction of secondary chemokine signals via "bystander" uninfected hepatocytes and that these immune cells would eliminate the *Plasmodium*-infected hepatocytes through some unknown mechanism (Gazzinelli et al., 2014; Liehl et al., 2014). In contrast to these notions, utilizing a Cre recombinase expressing *Plasmodium* strain capable of selectively ablating type I IFN signaling in the infected hepatocytes alone, we show that type I IFNs signaling in the infected hepatocytes is instrumental in the control of malaria. This finding should encourage additional research into potential IFN-induced cell-autonomous immune mechanisms targeting *Plasmodium* in hepatocytes and stimulate novel therapeutic opportunities and vaccination strategies against malaria.

RESULTS

Type I IFN signaling evident in *Plasmodium*-infected hepatocytes

It is well established that type I IFNs are critical for controlling *Plasmodium* infection in the liver and that systemic induction of adequate type I IFN responses limit *Plasmodium* development in the liver (Figures 1A and 1B) (Gazzinelli et al., 2014; Liehl et al., 2014; Miller et al., 2014). However, a direct role for type I IFNs in targeting *Plasmodium* or *Plasmodium*-infected hepatocytes had been previously ruled out based on the observation that treatment of *P. berghei*-infected primary hepatocytes with the drug DMXAA—a potent inducer of type I IFNs—did not impact *Plasmodium* development *in vitro* (Liehl et al., 2014). However, DMXAA treatment induces type I IFNs in mouse cells primarily through the stimulation of the cytosolic receptor stimulator of IFN genes (STING) (Conlon et al., 2013). STING is, however, not expressed in hepatocytes (Thomsen et al., 2016). Therefore, DMXAA treatment would not have induced type I IFNs in primary hepatocyte cultures. Of note, *Plasmodium* nucleic acids, which can potentially stimulate STING, are known to gain access to the cytosol of infected hepatocytes (Marques-da-Silva et al., 2021; Ni et al., 2018; Slavik et al., 2021). Yet, genetic deficiencies of STING or its signaling partner cGAS did not affect *Plasmodium* control in the liver, further supporting the absence of STING signaling in hepatocytes and its direct relevance to liver-stage malaria (Figure S1A). In contrast, direct IFNα and IFNβ (IFNα/β) treatment of *P. falciparum*-infected human primary hepatocytes or *P. berghei*-infected murine primary hepatocytes induced a significant and dose-dependent control of the infections (Figures 1C, 1D, and S1B). These findings renewed our interest in the possibility that type I IFNs played a direct role in controlling *Plasmodium* infection in hepatocytes.

Considering that a variety of IFN-induced genes and pathways are known to facilitate cellular responses that help eliminate intracellular pathogens (McNab et al., 2015), we hypothesized that autocrine or paracrine type I IFN signaling in hepatocytes would drive the clearance of *Plasmodium* from hepatocytes. In support of this premise, we observed IRF9 translocation into the nuclei of *P. berghei*-infected as well as the neighboring uninfected

cells in the liver of *P. berghei*-infected mice (Figures 1E and S1C). These data indicated that active type I IFN signaling is present in the vicinity of *Plasmodium*-infected hepatocytes (MacMicking, 2012).

To gain an unbiased view of the transcriptional changes induced by *Plasmodium* infection in primary hepatocytes, we performed microarray analysis of *P. berghei*-infected or uninfected hepatocytes (Figure S1D). We observed that while various biosynthetic and immune signaling pathways were impacted in *P. berghei*-infected hepatocytes, the majority of the transcriptional changes pertinent to pathogenesis and the disease process in such hepatocytes were associated with cell-death and inflammatory responses (Figures S1E and S1F). Intriguingly, a large number of type I IFN response genes were also concurrently perturbed in the hepatocytes in culture, following *P. berghei* infection (Figures 1F and 1G). This strengthened the premise that type I IFN signaling is active in *Plasmodium*-infected hepatocytes.

Type I IFN signaling in the infected hepatocytes controls *Plasmodium* infection

To determine the extent to which type I IFN signaling in infected hepatocytes contributed to the overall control of liver-stage malaria, we sought to negate type I IFN signaling solely in the infected hepatocytes. To this end, we generated a strain of *P. berghei*, *Pb-Cre*, which expresses and exports Cre recombinase into infected host hepatocytes wherein it would excise DNA sequences flanked by locus of X-over P1 (*loxP*) sites (“floxed”). *Pb-Cre* parasites were generated by fusing Cre recombinase with an SV40 nuclear localization signal (NLS) and a hemagglutinin (HA) tag on the C terminus of Lisp2 by CRISPR-mediated insertion of these coding sequences in the endogenous *pblisp2* genomic locus (Figure S2A). Lisp2 protein is expressed only by the *bona fide* liver stages of *Plasmodium* (i.e., exoerythrocytic forms [EEFs]) present in hepatocytes and is known to be transported across the parasitophorous vacuolar membrane into the hepatocyte cytosol (Gupta et al., 2019; Orito et al., 2013; Woodard et al., 2010). Therefore, the fusion with Lisp2 would limit Cre expression to the EEFs alone and facilitate its transport into the hepatocyte cytosol, where the SV40 NLS would drive its import into the host hepatocyte nucleus (Figure S2B). The levels of detectable Cre protein in *Pb-Cre*-infected hepatocyte cultures increased with time, supporting the notion that the establishment of liver-stage infection enables Cre expression in hepatocytes (Figure S2C).

To demonstrate the extent to which *Pb-Cre* can ablate target DNA sequences in host hepatocytes, we infected primary hepatocytes derived from Ai14 mice (Ai14 hepatocytes) with *Pb-Cre*. Ai14 mice possess a floxed STOP cassette preventing the transcription of a CAG promoter-driven red fluorescent protein variant, tdTomato (Madisen et al., 2010). Upon excision of the STOP cassette, tdTomato expression is “turned on” in Ai14 cells. Ai14 hepatocytes infected with *Pb-Cre* showed robust tdTomato expression (Figure S2D), indicating that *Pb-Cre* can be reliably used to ablate floxed target DNA sequences in *Plasmodium*-infected cells. Of note, primary hepatocytes derived from uninfected Ai14 mice exhibited very low baseline tdTomato expression (Figure S2E). Also, we failed to detect any tdTomato signal over background levels in non-parenchymal liver cells (i.e., the non-hepatocytes such as the hepatic myeloid cells) derived from *Pb-Cre*-infected Ai14 mice

(Figure S2F), although we have shown that such cells can acquire *Plasmodium* during the liver-stage of malaria (Kurup et al., 2019). This is likely because *Pb-Cre* would have to establish an infection in host cells and Cre exported to the host cell nucleus to induce the excision of floxed genes or gene fragments. Both of these are unlikely to occur in non-hepatocytes that scavenge the parasite without being actively infected. Therefore, *Pb-Cre* provided an opportunity to determine the relevance of specific genes in the host hepatocytes alone in the overall biology of *Plasmodium* infection.

To investigate how type I IFN responses specifically in the *Plasmodium*-infected hepatocytes impacted the control of liver-stage malaria, we utilized Ifnar1^{fl} mice, in which exon 3 of type I IFN α/β receptor (IFNAR1) is flanked by *loxP* sequences (Kamphuis et al., 2006). *Pb-Cre* infection induced disruption of the *Ifnar1* gene and resulted in tangible loss of IFNAR1 expression on Ifnar1^{fl} hepatocytes (Figures S2G and 2A). Of note, the time window available to observe the complete loss of any such gene expression in hepatocytes is limited by the ~48-h lifespan of *Plasmodium* development in mouse hepatocytes. However, even partial reduction in gene expression in parenchymal cells achieved using tools such as small interfering RNA (siRNA) has provided groundbreaking advancements in our understanding of host gene functions in a variety of liver diseases, including in malaria (Canal et al., 2015; Liehl et al., 2014; Rudalska et al., 2014). Compared with the control B6 hepatocytes, Ifnar1^{fl} hepatocytes failed to optimally control *Pb-Cre* infection *in vitro* (Figures 2B and S2H). This outcome was also noticed *in vivo*, where, compared with control B6 mice, Ifnar1^{fl} mice failed to limit *Pb-Cre* infection in the liver, even with systemic induction of type I IFNs through the administration of DMXAA (Figure 2C). Systemic delivery of DMXAA in mice is known to induce type I IFNs through the stimulation of STING in a variety of cell types such as the dendritic cells and macrophages (Curran et al., 2016). Sufficient administration of exogenous IFNα/β during the liver stage also significantly limited the progression *Pb-Cre* to blood-stage infection in the B6, but not the Ifnar1^{fl} mice (Figure 2D), revealing the relevance of intact type I IFN signaling in *Plasmodium*-infected hepatocytes in determining clinical outcomes. Of note, we observed patent parasitemia in one B6 mouse treated with IFNα/β, albeit being delayed until 8 days post infection. The experiment shown in Figure 2D was terminated at the 10-days post infection (p.i.) time point when B6 mice infected with *Pb-Cre* showed signs of cerebral malaria. Also, we relied on exogenous IFNα/β, as opposed to DMXAA, in the above experiment to minimize any potential direct impact the type I IFNs may have on *Plasmodium* blood stage; IFNα/β are known to have extremely short half-lives in mice (McKenna et al., 2004). The above findings indicated that type I IFN signaling in *Plasmodium*-infected hepatocytes is instrumental in limiting malaria. It is noteworthy, however, that liver-parasite burdens in *Pb-Cre*-infected Ifnar1^{fl} mice were similar to those in *Pb-Ova* (*P. berghei* transgenically expressing ovalbumin)-infected Ifnar1^{fl}-AlbCre mice, which lack IFNAR in all its hepatocytes (Liehl et al., 2014) (Figure 2C). This finding implied that the contribution of type I IFN signaling in uninfected hepatocytes of the liver in the control of malaria may be negligible. Taken together, these data indicated that type I IFN signaling in *Plasmodium*-infected hepatocytes is both necessary and sufficient to bring about IFN-mediated control of malaria in the liver.

The induction of tdTomato expression in Ai14 hepatocytes by *Pb-Cre* infection presented the unique opportunity to identify infected hepatocytes without relying on the detection of

proteins expressed by the parasite. Given that Cre-based activation of tdTomato expression in infected Ai14 hepatocytes is permanent, this system also enabled the identification of previously infected hepatocytes that may have cleared *Pb-Cre* infection. Surprisingly, a large number of Ai14 hepatocytes co-incubated with *Pb-Cre in vitro* expressed tdTomato without the presence of detectable parasites in them (Figures 2E, 2F, and S2I). Considering that only *bona fide* liver stages of *Pb-Cre* would express Cre, this suggested that the majority of hepatocytes infected with *Pb-Cre* may have eliminated the infection. Furthermore, Cre recombinase remained detectable in the majority of tdTomato expressing hepatocytes, suggesting that *Pb-Cre* was likely available in these cells, at some point. It is noteworthy, however, that some hepatocytes, which are possibly in their early stages of *Pb-Cre* infection, do not show detectable levels of Cre or tdTomato expression (Figures 2E and S2I). This is expected, considering that Lisp2 expression is limited to the mid-late merozoite stage of *Plasmodium* in the hepatocytes (Gupta et al., 2019; Orito et al., 2013).

There is the minor possibility that Ai14 hepatocytes may have acquired Cre recombinase from its environment (for example, from *Pb-Cre*-infected hepatocytes that underwent cell death) resulting in tdTomato expression rather than as a consequence of *Pb-Cre* infection itself. To test for this possibility, we performed a transwell-based assay where B6 or Ai14 hepatocytes were co-incubated with *Pb-Cre* in the upper chamber, separated from Ai14 hepatocytes in the lower chambers by pores of 0.4-μM diameter. This would allow the culture media containing any extracellular Cre recombinase to equilibrate but would prevent *Pb-Cre* sporozoites from accessing the Ai14 hepatocytes in the lower chamber (Figure S2J). Ai14 hepatocytes in the lower chambers showed no discernable tdTomato expression, indicating that *Pb-Cre* infection itself in Ai14 hepatocytes is necessary for Cre expression and is predominantly responsible for the induction of tdTomato expression (Figure S2K). In addition, these data also indicated that the tdTomato expression observed in Ai14 cells co-incubated with *Pb-Cre* is also not spontaneous or background fluorescence. Taken together, our findings demonstrate that we can selectively ablate target genes in *Plasmodium*-infected hepatocytes under both *in vitro* and *in vivo* conditions and that type I IFN signaling specifically in the infected hepatocytes is instrumental in limiting *Plasmodium* infection. Our findings also imply that active cell-intrinsic immune mechanisms may be present in hepatocytes, limiting the onset and severity of malaria. Only future studies will provide insights into the mechanisms behind this important process.

DISCUSSION

We show that innate immune control of *Plasmodium* in its liver stage occurs through type I IFN signaling specifically in the infected hepatocytes and that the majority of the hepatocytes eliminate *Plasmodium* parasites in the liver without tangible contributions from uninfected hepatocytes or other immune cells. This challenges the existing paradigm in the field that type I IFNs produced by *Plasmodium*-infected hepatocytes stimulate uninfected hepatocytes to induce chemokine signals that recruit leukocytes from circulation, which would subsequently eliminate the infected hepatocytes (Gazzinelli et al., 2014; He et al., 2020; Liehl et al., 2014). Our findings suggest that direct type I IFN-mediated elimination of *Plasmodium* in hepatocytes occurs potentially through autocrine and/or paracrine signaling and that such control of *Plasmodium* in the liver can have a significant impact on the onset

and overall parasite burden in the ensuing blood stage of the infection. These observations signified the importance of type I IFN signaling in the infected hepatocytes in deciding clinical outcomes in malaria.

Our data also suggest that cell-intrinsic immune responses in hepatocytes are instrumental in eliminating *Plasmodium* from infected hepatocytes. Although type I IFNs are considered key drivers of immune responses induced by and in the immune cells, the roles of IFN-induced pathways in controlling infections in non-immune cell types, such as parenchymal cells, are increasingly being appreciated (Gaudet et al., 2021; MacMicking, 2012). Given that type I IFNs are the key drivers of innate immune control of *Plasmodium* in the liver, our work offers important insights into how *Plasmodium* infection is naturally limited in the liver. There is emerging evidence for type I IFN responses impeding anti-malarial vaccine efficacies as well as facilitating the elimination of dormant *P. vivax* hypnozoites in the liver capable of seeding relapsing malaria infections (Mancio-Silva et al., 2022; Minkah et al., 2019). Understanding how type I IFNs drive the elimination of *Plasmodium* from the infected hepatocytes will provide key insights into the mechanisms enabling these processes. Our findings provide a robust platform to investigate type I IFN signaling, as well as the potential cell-autonomous immune mechanisms it might stimulate in the hepatocytes, to bring about natural immune control of malaria.

Limitations of the study

An infective mosquito bite is estimated to deliver approximately 123 sporozoites (with a range of 0–1,297) in mice (Medica and Sinnis, 2005). To determine the transmission of *Plasmodium* to blood stage, we therefore used an inoculum of 200 sporozoites. However, it is technically challenging to detect *Plasmodium* in the liver when infections are initiated with such low numbers of sporozoites. Therefore, it is necessary to use higher ($2–3 \times 10^4$) sporozoite doses to reliably detect *Plasmodium* burdens in mouse livers. There is a possibility that *Pb-Cre* infection may not have induced uniform deletion of the IFNAR1 gene or the complete loss of IFNAR protein expression in all infected hepatocytes. However, reducing protein expression has often produced tangible phenotypic outcomes, providing valuable information about the functional roles of targeted genes in hepatocytes. (Canal et al., 2015; Liehl et al., 2014; Rudalska et al., 2014). Therefore, we anticipate *Pb-Cre* to serve as an important tool to dissect the contributions of any hepatocyte gene toward anti-malarial immunity going forward.

STAR★METHODS

RESOURCE AVAILABILITY

Lead contact—Further information and requests for resources and reagents should be directed to the lead contact, Samarchith Kurup (samar@uga.edu).

Materials availability—Materials generated in this study are available upon reasonable request to the lead contact.

Data and code availability—Microarray data has been deposited to NCBI Gene Expression Omnibus and is publicly available. The accession number is listed in the key resources table. This paper does not report original code. Any additional information required to reanalyze the data reported in this paper is available from the lead contact upon request.

EXPERIMENTAL MODEL AND SUBJECT DETAILS

Mice—C57BL/6 (B6), Ai14 mice, Alb-Cre and Ifnar1^{fl} mice were procured from Jackson Laboratories. cGAS KO and STING KO mice were provided by Dr. Rick Tarleton (University of Georgia). Mice of either sex and 4-6 weeks of age were used to initiate the studies and were bred and housed with appropriate biosafety containment at the animal care units at the University of Georgia. The animals were treated and handled in accordance with guidelines established by the UGA Institutional Animal Care and Use Committees.

Parasites—Luciferase expressing *P. berghei* (*Pb-Luc*) were obtained from UGA *SporoCore*. We generated *Pb-GFP*, *Pb-Cre* and *Pb-Ova* transgenic parasites. For infections, salivary glands of parasitized *A. stephensi* mosquitos were dissected and sporozoites (spzs) were isolated as previously described (Kurup et al., 2019) and inoculated into cultures or injected intravenously ($2x10^4$/mouse) in 200μL total volume. P. berghei parasites (ANKA strain) were used to generate Pb-Cre and Pb-Ova parasites. Transfection, selection, and cloning of Pb-Cre were performed as described in detail before (Janse et al., 2006; Kurup et al., 2019). In short, *in vitro* cultured schizont stages of *P. berghei* were transfected with the target plasmids using Amaxa parasite nucleofection kit II (Lonza), by employing the manufacturer's protocol. The transgenic parasites were then inoculated into B6 mice and selected using pyrimethamine treatment. *A. stephensi* mosquitos infected with *P. berghei* ANKA, *Pb-Ova* and *Pb-Cre* were maintained at the University of Georgia insectary.

Primary hepatocytes—Both mouse and human primary hepatocytes used in this study were obtained as described in detail below. In short, the murine hepatocytes were purified from male or female mice, aged 4-6 weeks. Deidentified human hepatocytes were obtained from BioIVT, which is a commercial repository, and handled as described in detail below.

METHOD DETAILS

***P. falciparum* gametocyte culture and mosquito infection—**Gametocyte culture and mosquito infections were performed by modifying published protocols (Pathak et al., 2018). *P. falciparum* field isolate (CB132), was cultured with cryopreserved RBCs (Interstate Blood Bank). Briefly, asexual and gametocyte cultures were maintained at 38°C with 5% O_2 and 5% CO_2 gas composition in an O_2/CO_2 incubator (Panasonic). The culture received daily media change with RPMI 1640 + L-Glutamine + 25mM Hepes + 50 ug/mL hypoxanthine (KD Medical) and 5% heat-inactivated pooled human serum (Interstate Blood Bank). The asexual culture was kept between 0.5% to 5% parasitemia, and gametocyte culture was seeded at 0.5% parasitemia with cryopreserved O^+ human RBCs (5% hematocrit). Gametocyte culture was assessed for exflagellation using a hemocytometer (INCYTO) to count the number of exflagellation centers between 12-18 days post-seeding. Once deemed infectious during 12-18 days post-seeding, the cultures were offered to

150-250 3-7 days old female *Anopheles stephensi* mosquitoes as published before (Pathak et al., 2018). Infected mosquitoes were kept at 20°C ± 6°C, 80% ± 5% relative humidity, and under a 12-h day/night photoperiod schedule (Percival Scientific) with 5% dextrose (w/v) and 0.05% para-Aminobenzoic acid (w/v) (Thermo Fisher). Mosquito oocysts were checked at 10-days post-infection, and salivary glands were collected between 30-35 days post-infection.

Generation of Pblisp2 CRISPR-RGR plasmid—A CRISPR-RGR plasmid for the insertion of Cre recombinase, SV40 NLS, and a 1xHA tag was created using pSL1394 as a base plasmid (Addgene # 129522). A homology-directed repair (HDR) template was constructed that consists of: 1) a 5′ homology arm (5′ HA) comprising 411bp of the 3′ end of the *pblisp2* coding sequence, 2) coding sequence for a 2x(GGS) flexible linker, Cre, SV40 NLS, a single HA tag, and a stop codon, and 3) a 3′ homology arm (3′ HA) comprising 306bp of the sequences immediately downstream of *pblisp2*. Additionally, a Ribozyme-Guide-Ribozyme sequence was synthesized as previously described (Walker and Lindner, 2019) that expressed two sgRNAs with perfect homology to the targeted region of *pblisp2*. Distinct and unique promoter and 3′UTR sequences were used for each transcriptional cassette to avoid recombination and removal of *Plasmodium* sequences in the plasmid.

Murine primary hepatocyte culture, *in vitro* sporozoite infection—Primary hepatocytes were isolated from mice as described in detail before (Kurup et al., 2019). In short, in anesthetized (Ketamine/Xylazine (87.5/12.5 mg/Kg)) mice, the inferior vena cava was catheterized (BD auto guard, 22G) aseptically to perfuse the liver by draining the perfusate through the portal vein. A steady-state perfusion of the liver was performed first with PBS (4mL/min for 5 min), then Liver Perfusion buffer (4mL/min for 3 min, Gibco), and finally the Liver Digest Medium (4mL/min for 5 min, Gibco). Digested liver was excised, single cell suspension made and resuspended in a wash solution of 10% v/v fetal calf serum (Sigma-Aldrich) in DMEM (Gibco). Hepatocyte fraction was recovered by centrifugation at 57g, from which debris and dead cells were removed by density gradient centrifugation using a 46% v/v Percoll (Sigma) gradient. Remaining cells were counted and resuspended in DMEM with 10% v/v FCS. Primary hepatocytes cultures were plated for 24 h before infection. For luminescence measurement, 12 x 10^3 cells were plated on collagen-coated 96-well plates in 50μL volume and incubated at 37°C, and 5% CO_2, and then infected with 8 x10^3 sporozoites per well. Cultures were further incubated for 24-36 h to allow infection and liver-stage parasite development. Hepatocytes were stimulated with equal amounts of both murine IFNα and IFNβ (PBL) at varying concentrations, 1U = 0.8pg.

***P. falciparum* liver-stage infection—**Primary human hepatocyte infection in this study followed published methods (Roth et al., 2018). Briefly, cryopreserved primary human hepatocytes (BioIVT) were thawed two days prior to infection and seeded with 18,000 cells per well in a 384-well collagen-coated plate (Greiner). Hepatocyte cultures were maintained with daily media change with customized InVitroGro HI medium without dexamethasone (BioIVT) supplemented with 5% human serum (Interstate Blood Bank), 1:100 dilution of penicillin/streptomycin/neomycin antibiotic mixture (Gibco), and 1:1000 dilution of

gentamicin (stock concentration:10 mg/mL, Gibco). The salivary glands of *P. falciparum* BD007 infected *A. stephensi* mosquitoes were collected between 18-20 days post-infection and were passed through a 30-gauge needle (Becton Dickinson). Total sporozoites were determined using a hemocytometer, and 24,000 sporozoites were inoculated into the hepatocyte culture. The plate was centrifugated at room temperature at 250 *rcf* for 5 min with acceleration/break at 5. Hepatocyte cultures were kept at 38°C with 5% CO_2 (Panasonic). These cultures were treated with human IFN_α and IFN_β (PBL Assay Science) at varying concentrations, 1U = 3.6pg.

Assessment of parasite burdens—Liver parasite burdens were assessed by quantitative real-time RT-PCR for parasite 18s rRNA in hepatocytes derived from mice challenged with *Plasmodium* sporozoites, as described before (Doll et al., 2016; Kurup et al., 2019). Total RNA was extracted from hepatocytes at the indicated time points post infection, using TRIzol (Sigma Aldrich) treatment, followed by DNase digestion, and cleanup with RNA Clean and Concentrator kit (Zymo Research). Two micrograms of liver RNA per sample was used for qRT-PCR analysis for *Plasmodium* 18S rRNA using TaqMan Fast Virus 1-Step Master Mix (Applied Biosystems). Data were normalized for input to the GAPDH control (hepatocytes) for each sample and are presented as ratios of *Plasmodium* 18s rRNA to host GAPDH RNA. Data were normalized between experiments if appropriate, using naïve samples. Please see the key resources table for the primer sequences. The ratios depict relative parasite loads within an experiment and do not represent absolute values.

Blood stage parasitemia was assessed by flow cytometry as described before (Kurup et al., 2017). In the indicated time points, whole blood samples were stained with Hoechst 33342 (Sigma), anti-Ter119 coupled to Phycoerythrin (PE) (Tonbo Biosciences), and anti-CD45 coupled to allophycocyanine (APC) (Tonbo Biosciences). Data were acquired on Cytoflex (Beckman Coulter) and analyzed using FlowJo X (Treestar).

The frequencies of *P. berghei*-infected hepatocytes *in vitro* were determined with CellTrace violet (CTV, Thermofisher) stained sporozoites and flow cytometry. Sporozoites were stained with CTV by modifying the manufacturer's protocol, by incubating with 10mM CTV at 37°C for 20 min. The labeled sporozoites were then incubated for 5 min with 1mL FCS at 37°C to quench unbound CTV, washed once with media, and added to hepatocyte cultures.

Pb-Luc infection loads were determined using Bright-Glo (Promega) as described before (Derbyshire et al., 2012). In short, in a 96-well plate, after 16-h of infection, cells were treated or not with the indicated equal concentrations of IFNα and IFNβ for additional 20-h. 36-h post infection, Bright-Glo reagent was added and parasitemia evaluated. The relative signal intensity of each plate was evaluated with Synergy H4 hybrid reader (Biotek) and Gen 5 2.0 System.

P. falciparum liver stage quantification was performed by immunofluorescence microscopy at 4 days post-infection, and using with 5 technical replicates wells in a 384-well plate. Infected hepatocyte treated with varying concentration of IFN_α and IFN_β (1U = 3.6pg) at 16-h p.i. At 4d p.i., cultures were fixed with 4% v/v paraformaldehyde (Alfa Aesar) for

10 min at room temperature and washed twice with PBS followed by permeabilization, blocking and staining with 0.03% v/v Triton-X (Acros), 1% w/v BSA (w/v) (Fisher Scientific) and 1:1000 dilution of mouse anti-GAPDH (stock concentration 1mg/mL, European Malaria Reagent Repository, UK) overnight at 4°C. A secondary antibody mixture was made using the same permeabilization/blocking solution with 1:1000 dilution of anti-mouse Alexa Flour 488 (Thermo Fisher) overnight at 4°C. The wells were then stained with 10 μg/mL Hoechst (Sigma-Aldrich) under room temperature for 1 h. Fixed and stained samples were stored in PBS for quantification. The number of parasites in each well was imaged using ImageXpress and quantified using MetaXpress software (Molecular Devices). Images were acquired using FITC, and DAPI channels at 10X magnification, resulting in each well of a 384-well plate offering 9 fields of view, tiled together. After image acquisitions, hepatocyte nuclei were counted with the DAPI channel. Parasites were counted with the FITC channel and were identified by area, mean intensity, and cell roundness.

Flow cytometry and FACS—*Plasmodium* infection in RBC or hepatocytes were determined by flow cytometry as described in the 'assessment of parasite burdens' section above. The frequency of hepatocytes expressing tdTomato or IFNAR1 were determined using flow cytometry analysis of the hepatocytes. In short, to determine tdTomato expression, infected or not primary hepatocyte cultures were detached with trypsin (Corning), washed with RPMI and analyzed using flow cytometry (Cytoflex, Beckman Coulter and FlowJo X, Treestar).

To determine surface IFNAR expression in hepatocytes, the hepatocytes in culture were treated with trypsin, washed with RPMI, and analyzed by flow cytometry after staining with anti-IFNAR1 antibody. The data were acquired on Cytoflex (Beckman Coulter) and analyzed using FlowJo X (Treestar). Sporozoites were stained using CellTrace Violet (CTV) as described above, to delineate the infected hepatocytes from within the culture. Such CTV-stained hepatocytes were also flow-sorted (MoFlo Astrios EQ sorter, Beckman Coulter) to determine IFNAR1 transcripts in the infected (CTV^+) and currently uninfected (CTV^-) hepatocytes. $CD11c^+$ APCs harboring CTV^+ *Pb-Cre* were identified by flow-cytometry, following the protocol described before (Kurup et al., 2019). In short, the non-hepatocyte fraction of the mouse livers was enriched by centrifugation, stained with CD11c surface markers and analyzed using an Agilent Quanteon flow cytometer and analyzed using Flowjo X software (Treestar).

Trans-well assay—Primary hepatocytes derived from B6 or Ai14 mice were plated in the lower and/or upper chambers of a 12-well trans-well plate (0.4μm pore size) and the upper chamber cultures infected with *Pb-Cre* spzs. After 24 h of infection, cells from upper and lower chambers were trypsinized washed with RPMI and analyzed by flow-cytometry (Cytoflex, Beckman Coulter and FlowJo X, Treestar).

qPCR to determine IFNAR gene disruption—*Ifnar1* expression was assessed by quantitative real-time PCR in *Pb-Cre* infected (CTV^+) or uninfected (i.e., with undetectable parasite at the time, CTV^-) *in vitro* cultured primary hepatocytes. Total DNA was extracted from the flow-sorted infected or uninfected hepatocytes at 24-36 h post infection using PureLink Genomic DNA Mini Kit (Invitrogen) following the manufacturer's protocol. We

utilized an intronic forward primer coupled with a reverse primer targeting *Ifnar*1 exon 3 to determine the presence of intact *Ifnar1* gene. These primers were which were validated by the supplier of mice: Jax labs, and the sequences are available in the key resources table. Data were normalized for input using tumor necrosis factor (*Tnf*) gene as the control for each sample and data are presented as ratios of *Ifnar1* and *Tnf* genes. The *Pb-Cre* spzs were stained with CTV and the *Pb-Cre*-infected hepatocytes sorted, as described above.

Western blot for Cre recombinase—*Pb-Cre* infected cultured primary hepatocytes (1×10^6) at different time points were homogenized in 1% NP-40 lysis buffer with a cocktail of protease inhibitors (Roche) and resuspended in 1x Laemmli sample buffer (Bio-Rad) containing β-mercaptoethanol (Sigma-Aldrich). Equal amounts of proteins were separated by SDS-PAGE and Western blotting was performed as described before (Marques-da-Silva et al., 2021). The bands visualized by enhanced chemiluminescence assay using LICOR 800 as secondary antibody at 1:20,000 dilution and the images were acquired using a Chemidoc (Bio-Rad).

Therapeutic regimens—The following *in vivo* treatment regimens were used in this study: DMXAA (5,6-dimethylxanthenone-4- acetic acid, Invivogen): 20mg/Kg intraperitoneal (i.p.), 1d p.i. Poly I:C (Invivogen): 100ug/mouse, hydrodynamic i.v., 1dpi. Murine IFNα and IFNβ: 3.3μg/Kg i.p. 12-h p.i. and 24-h p.i.

Microscopy—*Plasmodium*-infected hepatocytes cultured (30-h p.i.) on collagen coated cover-slips were fixed with 4% paraformaldehyde in PBS for 10 min. The samples were washed with PBS and co-incubated with 0.25% v/v Triton X-100/PBS (Fisher Bioscience) for 10 min at room-temperature to permeabilize plasma membranes. Samples were subsequently blocked with 1% w/v BSA/PBS (60 min), stained with specific antibodies that delineate the PVM (anti-UIS4 or Hep17, in house generated), anti-IRF-9 (Clone 6F1-H5, Millipore Sigma), anti-HA (Clone 16B12, Biolegend) anti-Cre Recombinase (Clone poly9080, Biolegend) or 4′,6-Diamidino-2-Phenylindole, Dihydrochloride (DAPI, Sigma Aldrich) for 60 min. The samples were washed thrice with PBS, probed with fluorophore conjugated secondary antibodies, washed thrice with PBS again and visualized in Applied Precision DeltaVision Microscope System I (Olympus IX-71) and processed using SoftWorx software.

Transcriptome analysis—*Pb-GFP* infected or naïve (from uninfected cultures) hepatocytes derived from cultured prepared as described above were FACS sorted and re-suspended in TRIzol. RNA was purified with RNAeasy kit (Qiagen) as described previously (Vijay et al., 2017). RNA was assessed for purity and quality using an Agilent 2100 Bioanalyzer and transcriptome analysis performed on Affymetrix GeneChip Mouse Transcriptome array 1.0. Data output was analyzed and visualized using Affymetrix Expression Console v1.4.4.46, Applied Biosystems Transcription Analysis Console v4.0.1.36 and Interferome v2.01 (www.interferome.org) and submitted to NCBI Gene Expression Omnibus (GSE186023).

QUANTIFICATION AND STATISTICAL ANALYSES

Statistical differences between two study groups were evaluated using two-tailed t-tests. Statistical differences between more than two study groups were evaluated using ANOVA with the indicated corrections applied. Statistical significance was calculated based on the numbers of biological replicates as indicated in the figures or figure legends and assigned as *$p \leq 0.05$, **$p < 0.01$, n.s: $p > 0.05$. Statistical analyses were performed using Prism 9 software (GraphPad) and on combined data from replicate experiments and are as indicated in the respective figure legends.

Supplementary Material

Refer to Web version on PubMed Central for supplementary material.

ACKNOWLEDGMENTS

We want to acknowledge the contributions of Dr. John Harty (University of Iowa) for offering vital insights pertinent to the study and critiquing the manuscript. We Dr. Rick Tarleton (University of Georgia) for vital resources and critiquing the manuscript. We acknowledge the contributions of UGA Office of animal research, the UGA CTEGD central microscopy core, the UGA CTEGD central flow core, and Iowa Institute of Human Genetics for providing valuable access to their facilities, as well as the technical support provided by Drs. Diego Huet (UGA) and Ronald Etheridge (UGA). Graphics were generated using BioRender. The study was supported by NIH R21AI130692 to S.E.L., NIH R21AI144591 to D.E.K., T32AI1060546 to J.S., and UGA research startup to S.P.K.

REFERENCES

Canal F, Anthony E, Lescure A, Del Nery E, Camonis J, Perez F, Ragaz-zon B, and Perret C (2015). A kinome siRNA screen identifies HGS as a potential target for liver cancers with oncogenic mutations in CTNNB1. BMC Cancer 15, 1020. 10.1186/s12885-015-2037-8. [PubMed: 26715116]

Conlon J, Burdette DL, Sharma S, Bhat N, Thompson M, Jiang Z, Ra-thinam VAK, Monks B, Jin T, Xiao TS, et al. (2013). Mouse, but not human STING, binds and signals in response to the vascular disrupting agent 5, 6-dimethylxanthenone-4-acetic acid. J. Immunol 190, 5216–5225. 10.4049/jimmunol.1300097. [PubMed: 23585680]

Cowman AF, Healer J, Marapana D, and Marsh K (2016). Malaria: biology and disease. Cell 167, 610–624. 10.1016/j.cell.2016.07.055. [PubMed: 27768886]

Curran E, Chen X, Corrales L, Kline DE, Dubensky TW Jr., Duttagupta P, Kortylewski M, and Kline J (2016). STING pathway activation stimulates potent immunity against acute myeloid leukemia. Cell Rep. 15, 2357–2366. 10.1016/j.celrep.2016.05.023. [PubMed: 27264175]

Derbyshire ER, Prudêncio M, Mota MM, and Clardy J (2012). Liver-stage malaria parasites vulnerable to diverse chemical scaffolds. Proc. Natl. Acad. Sci. USA 109, 8511–8516. 10.1073/pnas.1118370109. [PubMed: 22586124]

Doll KL, Pewe LL, Kurup SP, and Harty JT (2016). Discriminating protective from nonprotective plasmodium-specific CD8+ T cell responses. J. Immunol 196, 4253–4262. 10.4049/jimmunol.1600155. [PubMed: 27084099]

Gaudet RG, Zhu S, Halder A, Kim BH, Bradfield CJ, Huang S, Xu D, Mamiñska A, Nguyen TN, Lazarou M, et al. (2021). A human apolipoprotein L with detergent-like activity kills intracellular pathogens. Science 373, eabf8113. 10.1126/science.abf8113. [PubMed: 34437126]

Gazzinelli RT, Kalantari P, Fitzgerald KA, and Golenbock DT (2014). Innate sensing of malaria parasites. Nat. Rev. Immunol 14, 744–757. 10.1038/nri3742. [PubMed: 25324127]

Gupta DK, Dembele L, Voorberg-van der Wel A, Roma G, Yip A, Chuen-chob V, Kangwanrangsan N, Ishino T, Vaughan AM, Kappe SH, et al. (2019). The Plasmodium liver-specific protein 2 (LISP2) is an early marker of liver stage development. Elife 8, e43362. 10.7554/eLife.43362. [PubMed: 31094679]

He X, Xia L, Tumas KC, Wu J, and Su XZ (2020). Type I interferons and malaria: a double-edge sword against a complex parasitic disease. Front. Cell. Infect. Microbiol 10, 594621. 10.3389/fcimb.2020.594621. [PubMed: 33344264]

Janse CJ, Ramesar J, and Waters AP (2006). High-efficiency transfection and drug selection of genetically transformed blood stages of the rodent malaria parasite Plasmodium berghei. Nat. Protoc 1, 346–356. 10.1038/nprot.2006.53. [PubMed: 17406255]

Kamphuis E, Junt T, Waibler Z, Forster R, and Kalinke U (2006). Type I interferons directly regulate lymphocyte recirculation and cause transient blood lymphopenia. Blood 108, 3253–3261. 10.1182/blood-2006-06-027599. [PubMed: 16868248]

Kurup SP, Anthony SM, Hancox LS, Vijay R, Pewe LL, Moioffer SJ, Sompallae R, Janse CJ, Khan SM, and Harty JT (2019). Monocyte-derived CD11c(+) cells acquire Plasmodium from hepatocytes to prime CD8 T cell immunity to liver-stage malaria. Cell Host Microbe 25, 565–577.e6. 10.1016/j.chom.2019.02.014. [PubMed: 30905437]

Kurup SP, Obeng-Adjei N, Anthony SM, Traore B, Doumbo OK, Butler NS, Crompton PD, and Harty JT (2017). Regulatory T cells impede acute and long-term immunity to blood-stage malaria through CTLA-4. Nat. Med 23, 1220–1225. 10.1038/nm.4395. [PubMed: 28892065]

Liehl P, Zuzarte-Luís V, Chan J, Zillinger T, Baptista F, Carapau D, Ko-nert M, Hanson KK, Carret C, Lassnig C, et al. (2014). Host-cell sensors for Plasmodium activate innate immunity against liver-stage infection. Nat. Med 20, 47–53. 10.1038/nm.3424. [PubMed: 24362933]

MacMicking JD (2012). Interferon-inducible effector mechanisms in cell-autonomous immunity. Nat. Rev. Immunol 12, 367–382. 10.1038/nri3210. [PubMed: 22531325]

Madisen L, Zwingman TA, Sunkin SM, Oh SW, Zariwala HA, Gu H, Ng LL, Palmiter RD, Hawrylycz MJ, Jones AR, et al. (2010). A robust and high-throughput Cre reporting and characterization system for the whole mouse brain. Nat. Neurosci 13, 133–140. 10.1038/nn.2467. [PubMed: 20023653]

Mancio-Silva L, Gural N, Real E, Wadsworth MH 2nd, Butty VL, March S, Nerurkar N, Hughes TK, Roobsoong W, Fleming HE, et al. (2022). A single-cell liver atlas of Plasmodium vivax infection. Cell Host Microbe 30, 1–13. 10.1016/j.chom.2022.03.034. [PubMed: 35026130]

Marques-da-Silva C, Poudel B, Baptista RP, Peissig K, Hancox LS, Shiau JC, Pewe L, Shears MJ, Kanneganti T-D, Sinnis P, et al. (2021). Altered cleavage of Caspase-1 in hepatocytes limits control of malaria in the liver. Preprint at bioRxiv. 10.1101/2021.01.28.427517.

McKenna SD, Vergilis K, Arulanandam AR, Weiser WY, Nabioullin R, and Tepper MA (2004). Formation of human IFN-beta complex with the soluble type I interferon receptor IFNAR-2 leads to enhanced IFN stability, pharmacokinetics, and antitumor activity in xenografted SCID mice. J. Interferon Cytokine Res 24, 119–129. 10.1089/107999004322813363. [PubMed: 14980076]

McNab F, Mayer-Barber K, Sher A, Wack A, and O'Garra A (2015). Type I interferons in infectious disease. Nat. Rev. Immunol 15, 87–103. 10.1038/nri3787. [PubMed: 25614319]

Medica DL, and Sinnis P (2005). Quantitative dynamics of Plasmodium yoelii sporozoite transmission by infected anopheline mosquitoes. Infect. Immun 73, 4363–4369. 10.1128/IAI.73.7.4363-4369.2005. [PubMed: 15972531]

Miller JL, Sack BK, Baldwin M, Vaughan AM, and Kappe SH (2014). Interferon-mediated innate immune responses against malaria parasite liver stages. Cell Rep. 7, 436–447. 10.1016/j.celrep.2014.03.018. [PubMed: 24703850]

Minkah NK, Wilder BK, Sheikh AA, Martinson T, Wegmair L, Vaughan AM, and Kappe SHI (2019). Innate immunity limits protective adaptive immune responses against pre-erythrocytic malaria parasites. Nat. Commun 10, 3950. 10.1038/s41467-019-11819-0. [PubMed: 31477704]

Mo AX, and McGugan G (2018). Understanding the liver-stage biology of malaria parasites: insights to enable and accelerate the development of a highly efficacious vaccine. Am. J. Trop. Med. Hyg 99, 827–832. 10.4269/ajtmh.17-0895. [PubMed: 30141395]

Mo AXY, Pesce J, Augustine AD, Bodmer JL, Breen J, Leitner W, and Hall BF (2020). Understanding vaccine-elicited protective immunity against pre-erythrocytic stage malaria in endemic regions. Vaccine 38, 7569–7577. 10.1016/j.vaccine.2020.09.071. [PubMed: 33071001]

Ni G, Ma Z, and Damania B (2018). cGAS and STING: at the intersection of DNA and RNA virus-sensing networks. PLoS Pathog. 14, e1007148. 10.1371/journal.ppat.1007148. [PubMed: 30114241]

Orito Y, Ishino T, Iwanaga S, Kaneko I, Kato T, Menard R, Chinzei Y, and Yuda M (2013). Liver-specific protein 2: a Plasmodium protein exported to the hepatocyte cytoplasm and required for merozoite formation. Mol. Microbiol 87, 66–79. 10.1111/mmi.12083. [PubMed: 23216750]

Pathak AK, Shiau JC, Thomas MB, and Murdock CC (2018). Cryogenically preserved RBCs support gametocytogenesis of Plasmodium falciparum in vitro and gametogenesis in mosquitoes. Malar. J 17, 457. 10.1186/s12936-018-2612-y. [PubMed: 30522507]

Roth A, Maher SP, Conway AJ, Ubalee R, Chaumeau V, Andolina C, Kaba SA, Vantaux A, Bakowski MA, Thomson-Luque R, et al. (2018). A comprehensive model for assessment of liver stage therapies targeting Plasmodium vivax and Plasmodium falciparum. Nat. Commun 9, 1837. 10.1038/s41467-018-04221-9. [PubMed: 29743474]

Rudalska R, Dauch D, Longerich T, McJunkin K, Wuestefeld T, Kang TW, Hohmeyer A, Pesic M, Leibold J, von Thun A, et al. (2014). In vivo RNAi screening identifies a mechanism of sorafenib resistance in liver cancer. Nat. Med 20, 1138–1146. 10.1038/nm.3679. [PubMed: 25216638]

Slavik KM, Morehouse BR, Ragucci AE, Zhou W, Ai X, Chen Y, Li L, Wei Z, Bähre H, König M, et al. (2021). cGAS-like receptors sense RNA and control 3'2'-cGAMP signalling in Drosophila. Nature 597, 109–113. 10.1038/s41586-021-03743-5. [PubMed: 34261127]

Thomsen MK, Nandakumar R, Stadler D, Malo A, Valls RM, Wang F, Reinert LS, Dagnaes-Hansen F, Hollensen AK, Mikkelsen JG, et al. (2016). Lack of immunological DNA sensing in hepatocytes facilitates hepatitis B virus infection. Hepatology 64, 746–759. 10.1002/hep.28685. [PubMed: 27312012]

Vijay R, Fehr AR, Janowski AM, Athmer J, Wheeler DL, Grunewald M, Sompallae R, Kurup SP, Meyerholz DK, Sutterwala FS, et al. (2017). Virus-induced inflammasome activation is suppressed by prostaglandin D2/DP1 signaling. Proc. Natl. Acad. Sci. USA 114, E5444–E5453. 10.1073/pnas.1704099114. [PubMed: 28630327]

Walker MP, and Lindner SE (2019). Ribozyme-mediated, multiplex CRISPR gene editing and CRISPR interference (CRISPRi) in rodent-infectious Plasmodium yoelii. J. Biol. Chem 294, 9555–9566. 10.1074/jbc.RA118.007121. [PubMed: 31043479]

WHO. (2019). World Malaria Report 2019 (World Health Organization), pp. 1–232. citeulike-article-id:13565866.

Woodard LE, Hillman RT, Keravala A, Lee S, and Calos MP (2010). Effect of nuclear localization and hydrodynamic delivery-induced cell division on φC31 integrase activity. Gene Ther. 17, 217–226. 10.1038/gt.2009.136. [PubMed: 19847205]

Highlights

- Type I interferon (IFN) signaling in the infected hepatocytes controls malaria
- Cre recombinase expressing *Plasmodium* ablates target genes in infected hepatocytes
- The majority of the infected hepatocytes tend to naturally eliminate *Plasmodium* infection
- Such IFN-induced control of *Plasmodium* in the liver impedes blood-stage malaria

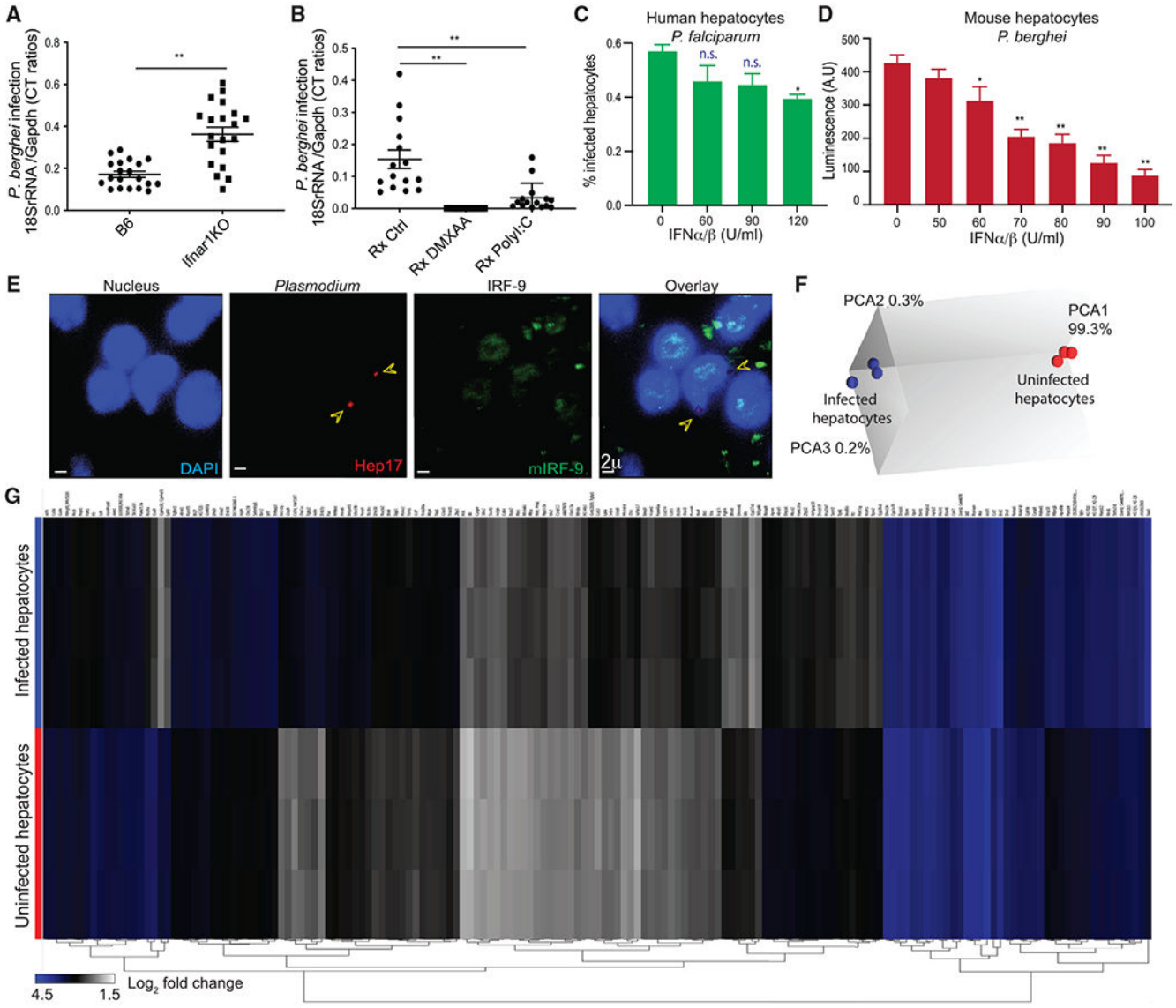

Figure 1. Type I interferon signaling in *Plasmodium*-infected hepatocytes

(A) Scatterplots showing relative liver-parasite burdens in B6 or Ifnar1 knockout (KO) mice inoculated with 3×10^4 *P. berghei* sporozoites (spzs) at 36-h post infection (p.i.).

(B) Scatterplots showing relative liver-parasite burdens in B6 mice treated with vehicle control, STING agonist DMXAA, or TLR3 agonist polyI:C (−1 day p.i.), and inoculated with 3×10^4 *P. berghei* spzs at 36-h p.i.

(A and B) Data points represent individual mice, presented as mean ± SEM and analyzed using two-tailed t test (A) or one-way ANOVA with Tukey's correction (B), and are combined from three separate experiments with ≥3 mice/group.

(C) Frequency of *P. falciparum*-infected primary human hepatocyte in cultures treated with the indicated concentrations of IFNα/β at 4 days p.i. Data are combined from three separate experiments with ≥3 technical replicates.

(D) Parasite loads indicated by luciferase activity in primary mouse hepatocyte cultures infected with firefly luciferase expressing *P. berghei (Pb-luc)* and treated with the indicated concentrations of IFNα/β at 36-h p.i. A.U., arbitrary units.

(C and D) Data are presented as mean ± SEM and analyzed using ANOVA comparing the indicated groups with the group treated with 0 U/mL IFNα/β. Data are normalized for background signal and combined from three separate experiments with ≥3 technical replicates.

(E) Representative (>10 fields) pseudo-colored confocal images depicting IRF-9 translocation into host cell nuclei, indicating type I IFN signaling in *P. berghei*-infected B6 mice liver (cryosection) at 24-h p.i. The arrows indicate *P. berghei* exoerythrocytic forms (EEFs) stained for Hep17 protein in the parasitophorous vacuolar membrane (PVM) in the infected hepatocytes.

(F) Principal-component analysis representing gross transcriptional differences between *P. berghei* (*Pb-GFP*)-infected primary murine hepatocytes sorted from infected cultures (36-h p.i.) and naive B6 hepatocytes from parallel uninfected *in vitro* cultures.

(G) Transcriptional perturbations in the interferon regulated genes of *P. berghei*-infected or uninfected hepatocytes isolated from *P. berghei*-infected or naive primary murine (B6) hepatocyte cultures at 36-h p.i.

(F) and (G) represent three replicate infections. *$p \leq 0.05$, **$p < 0.01$, n.s. $p > 0.05$.

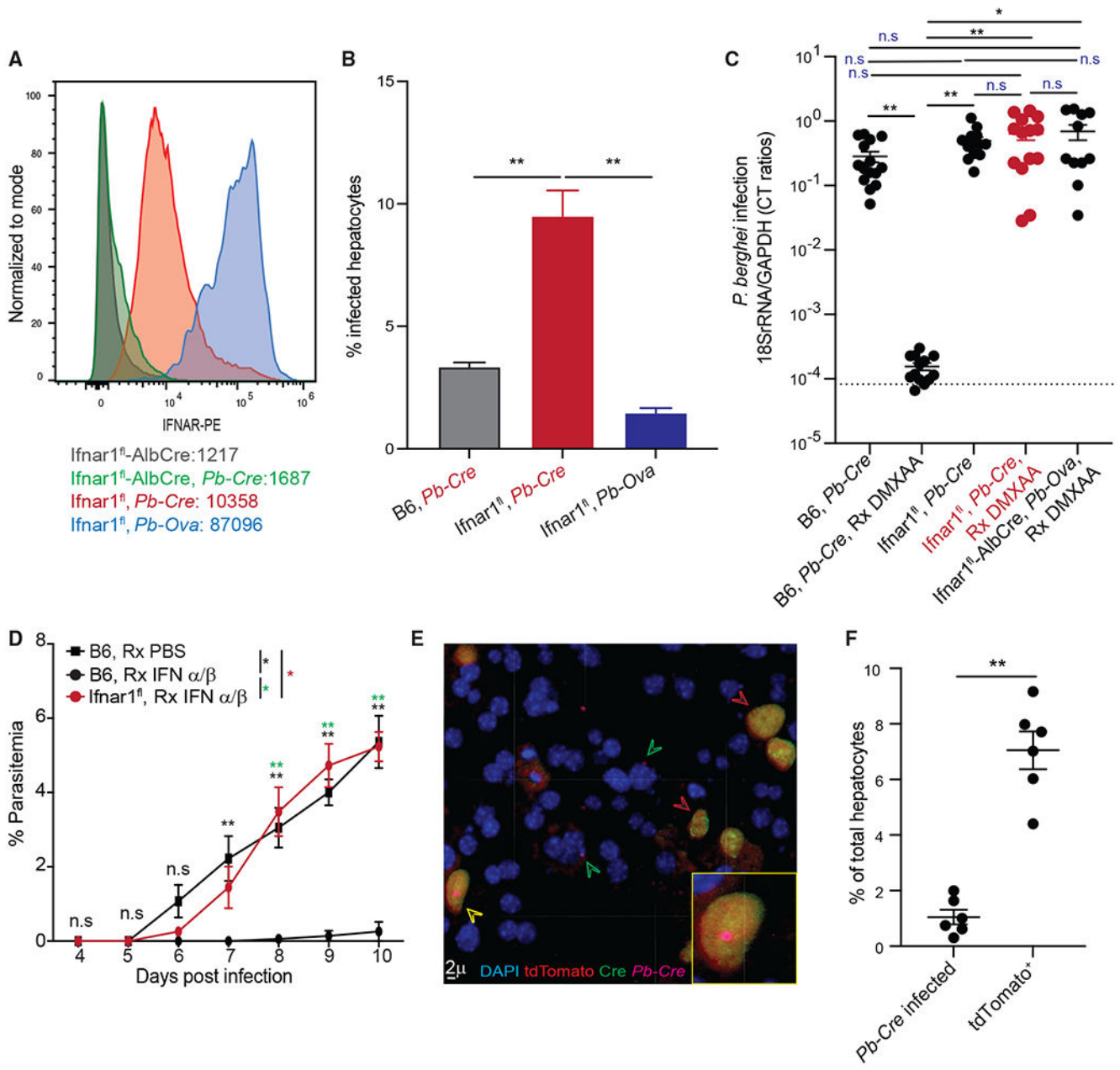

Figure 2. Type I IFN signaling in the infected hepatocytes controls malaria

(A) Histograms representing the expression levels of IFNAR in *Pb-Cre*-infected Ifnarl^{fl} hepatocytes at 36-h p.i. *Pb-Ova*-infected Ifnar1^{fl} hepatocytes, *Pb-Cre*-in-fected Ifnar1^{fl}-AlbCre, or uninfected Ifnar1^{fl}-AlbCre hepatocytes served as controls. The numbers indicate mean fluorescence intensities. Spzs were stained using CellTrace Violet (CTV) to identify the *Plasmodium*-infected hepatocytes from the infected cultures. Representative data are shown from one of three separate experiments.

(B) Frequencies of infected B6 or Ifnar1^{fl} primary hepatocytes in culture co-incubated with *Pb-Cre* or control *Pb-Ova* parasites at 36-h p.i. Combined data are presented as mean ± SEM from three experiments and are analyzed using one-way ANOVA with Tukey's correction.

(C) Scatterplots showing relative liver-parasite burdens at 36-h p.i. in the various groups of mice inoculated with 3×10^4 *Pb-Cre* or *Pb-Ova* spzs as indicated and treated with or without DMXAA at 24-h p.i. Combined data are presented as mean ± SEM from three experiments and are analyzed using one-way ANOVA with Tukey's correction. Dots represent individual mice. Dotted line indicates the mean background signal derived from two naive mice.
(D) Kinetics of parasitemia in the indicated groups of mice inoculated with 200 *Pb-Cre* spzs and treated with IFNα/β or control PBS at 12- and 24-h p.i. Combined data from three experiments are presented as mean ± SEM and are analyzed using two-way ANOVA with Tukey's correction.
(E) Representative (>10 fields) pseudo-colored confocal image indicating tdTomato expression, Cre localization, or *Pb-Cre* in primary Ai14 mouse hepatocytes in culture at 36-h p.i.; green arrows indicate *Pb-Cre* infection in hepatocytes, red arrows indicate tdTomato-expressing hepatocytes, and yellow arrow shows tdTomato-expressing cells that have detectable *Pb-Cre* ($Hep17^+$) parasites in them. Picture inset shows magnified image of a single *Pb-Cre*-infected hepatocyte with detectable *Pb-Cre* in it. See Figure S2H for individual channels.
(F) Scatterplot indicating the frequencies of primary Ai14 mouse hepatocytes exhibiting tdTomato expression or detectable infection when co-incubated with *Pb-Cre* spzs for 36 h. Combined data are presented as mean ± SEM and are analyzed using two-tailed t tests, with each dot representing data from a replicate experiment. *$p \leq 0.05$, **$p < 0.01$, n.s. $p > 0.05$.

KEY RESOURCES TABLE

REAGENT or RESOURCE	SOURCE	IDENTIFIER
Antibodies		
Anti-Ter119-PE	Tonbo Biosciences	Cat# 50-5921
Anti-CD45-APC	Tonbo Biosciences	Cat# 20-0451
Anti-UIS4	This paper	N/A
Anti-IRF-9	Millipore Sigma	Cat# MABS1920
Anti-Hep17	This paper	N/A
Anti-Cre recombinase	Biolegend	Cat# PRB-106P
Anti-mouse Alexa fluor 488	Thermo Fisher	Cat # A-10631
Anti-HA	Biolegend	Cat# MMS-101P
Anti-mouse beta tubulin	R&D Systems	Cat# MAB9344
Anti-mouse IFNAR1	Biolegend	Cat# 127311
Mouse anti-GAPDH	European Malaria Reagent Repository, UK	Cat# 13.3
Chemicals, peptides, and recombinant proteins N/A		
Triton X-100	Acros	Cat# 215680010
TaqMan Fast Virus 1-Step Master Mix	Applied Biosystems	Cat# 4444432
Bright-Glo	Promega	Cat# E2610
DAPI (2-(4-Amidinophenyl)-6-indolecarbamidine)	Sigma-Aldrich	Cat# D9542
Hoechst 33342	Sigma-Aldrich	Cat# H3570
Paraformaldehyde	Alfa Aesar	Cat# A11313
Bovine serum albumin	Fisher scientific	Cat# BP9700100
Pyrimethamine	Sigma-Aldrich	Cat# BP1227
Liver Perfusion Buffer	Gibco	Cat# 17701038
Percoll	Sigma-Aldrich	Cat# P1644
Liver Digestion Medium	Gibco	Cat# 17703034
Fetal Calf Serum	Sigma-Aldrich	Cat# 12106
DMEM	Gibco	Cat# 12430112
RPMI 1640, w/ l-glutamine + 25 mm hepes + 50mg/L hypoxanthine	KD Medical	Cat# CUS-0645
CellTrace Violet	Thermofisher	Cat# C34571
Para-Aminobenzoic Acid	ThermoFisher	Cat#150-13-0
Recombinant mouse IFNα	PBL Assay Science	Cat# 12100-1
Recombinant mouse IFNβ	PBL Assay Science	Cat# 12410-1
Recombinant human IFNα	PBL assay science	Cat#11101-1
Recombinant human IFNβ	PBL assay science	Cat# 11410-2
Penicillin-Streptomycin-Neomycin (PSN) Antibiotic	Gibco	Cat# 15640055
Gentamicin	Gibco	Cat# 15710072
Trypsin-EDTA	Corning	Cat# 25-051-CI
DMXAA	Invivogen	Cat# tlrl-dmx
Poly I:C	Invivogen	Cat# tlrl-pic

REAGENT or RESOURCE	SOURCE	IDENTIFIER
Invitrogro hi medium	BioIVT	Cat# Z990012
TRI reagent	Sigma-Aldrich	Cat# 93289
4x Laemmli protein sample buffer	Bio-Rad	Cat# 1610747
2-Mercaptoethanol	Sigma-Aldrich	Cat# M3148
Critical commercial assays		
Amaxa Parasite nucleofection kit	Lonza	Cat# VVMI-1011
RNA Clean and Concentrator Kit	Zymo research	Cat# R1019
RNeasy Kit	Qiagen	Cat# 74004
PureLink Genomic DNA Mini Kit	Invitrogen	Cat# K182001
Deposited data		
Microarray analysis data	NCBI Gene Expression Omnibus	GEO: GSE186023
Experimental models: Organisms/strains		
Plasmodium berghei-luciferase expressing	University of Georgia-Sporocore	N/A
P. berghei, GFP expressing (*Pb-GFP*)	This paper	N/A
P. berghei, Cre expressing (*Pb-Cre*)	This paper	N/A
P. berghei, Ovalbumin expressing (*Pb-Ova*)	Kurup CHM paper	PMID: 30905437
Anopheles stephensi	University of Georgia-Sporocore	N/A
Human RBCs	Interstate Blood Bank	N/A
Human hepatocytes	BioIVT	Cat#: M00995-P
P. falciparum	Field isolate/ D. Kyle	CB132
Mouse: C57BL/6	The Jackson laboratories	Strain#: 000664
Mouse: Ai14	The Jackson laboratories	Strain#: 007914
Mouse: IfngKO	The Jackson laboratories	Strain#: 002287
Mouse: Alb-Cre	The Jackson laboratories	Strain#: 003574
Mouse: Ifnar1^{flox}	The Jackson laboratories	Strain#: 028256
Mouse: Ifnar1^{flox} Alb-Cre	University of Georgia	N/A
Mouse: cGAS KO	University of Georgia/ R. Tarleton	N/A
Mouse: STING KO	University of Georgia/ R. Tarleton	N/A
Oligonucleotides		
TNF: 5′-CAG CAA GCA TCT ATG CAC TTA GAC CCC -3′; 5′-TCC CTC TCA TCA GTT CTA TGG CCC– 3′	Thermo-Fisher	N/A
IFNAR1: 5′ -ACT CAG GTT CGC TCC ATC AG -3′; 5′- CTT TTA ACC ACT TCG CCT CGT -3′	Thermo-Fisher	N/A
Pb: 5′- CGCAAGCGAGAAAGTTAAAAGAA-3′; 5′- GAGTCAAATTAAGCCGCAAGCT3′	IDT DNA	N/A
GAPDH: 5′ ACC ACA GTC CAT GCC ATC AC-3′; 5′- TCC ACC ACC CTG TTG CTG TA-3′	IDT DNA	Cat# 51-01-07-12/ 51-01-07-13
Recombinant DNA		
CRISPR-RGR plasmid	Addgene	#129522

REAGENT or RESOURCE	SOURCE	IDENTIFIER
Softwares and algorithms		
Ingenuity Pathway Analysis	Qiagen	V1-20-04
Bio Rad CFX Manager	Bio-Rad	V3.1
Expression Console	Affymetrix	V1.4.4.46
Gen 5 System	Biotek	V2.0
Image Lab Touch	Bio-Rad	V3.0.1
Cyt Expert	Beckman Coulter	V2.5
MetaXpress software	Molecular Devices	V6.6.3.55
Summit	Beckman Coulter	V62
Transcription Analysis Console	Applied Biosystems	V4.0.1.36
Interferome	www.interferome.org	V2.01
Prism	Graphpad	V9.3.1
FlowJo	Treestar	X
Biorender	Biorender.com	2022
Imaris	Bitplane	V9
Other		
Human serum	Interstate Blood Bank	N/A